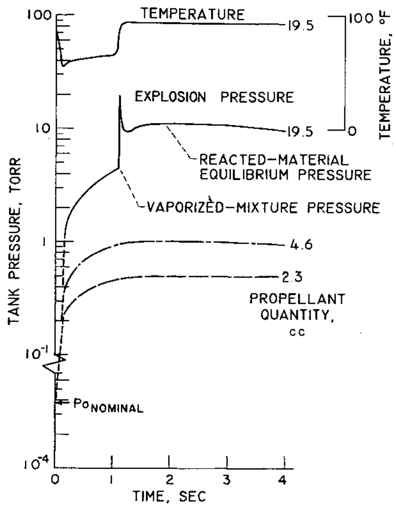

Fig. 1 Effect of varying propellant quantity on tank pressure rise.

propellant vaporization, which indicates that there was no reaction. With larger quantities of propellants (19.5 cm^3), the initial pressure rise (to the "vaporized-mixture-pressure" point) again could be predicted with complete vaporization assumed. This pressure rise was followed by an explosion pressure fluctuation that occurred when the tank pressure exceeded 4 Torr. The tank pressure ultimately reached a new equilibrium value. As expected, the transient temperature variations show a sharp decrease during propellant vaporization and a sharp rise during the reaction phase. The gradual temperature rise in between was caused by radiant energy from photographic flood lamps. It was apparent from the motion-picture film that the magnitude of the temperature decrease was sufficient to cause freezing of droplets of hydrazine on the capsule support mechanism. Later tests with single capsules of either N_2H_4 or N_2O_4 confirmed the fact that this freezing phenomenon occurred only in the N_2H_4.

Figure 2 shows the change in pressure-time history for various initial tank pressures p_0. In all cases, the reaction occurred at vaporized-mixture pressures greater than 4 Torr. Comparison of the three curves indicates a large reaction delay time for $p_0 = 1$ Torr, whereas for $p_0 = 6 \times 10^{-4}$ and 10^{-1} Torr, the reaction occurred after approximately 0.9 sec, and 2.25 sec were required at $p_0 = 1$ Torr. In addition, the sudden increase in pressure associated with explosion did not occur for an initial ambient pressure of 1 Torr; rather, the pressure increased smoothly from the vaporized-mixture to the reacted-material equilibrium pressure. Evidently, the region from 10^{-1} to 1 Torr is a transition region in which a less violent reaction occurs. Increasing ambient pressure increases the amount of inert gas (nitrogen) in the tank; thus the dilution of the propellant may explain this phenomenon.

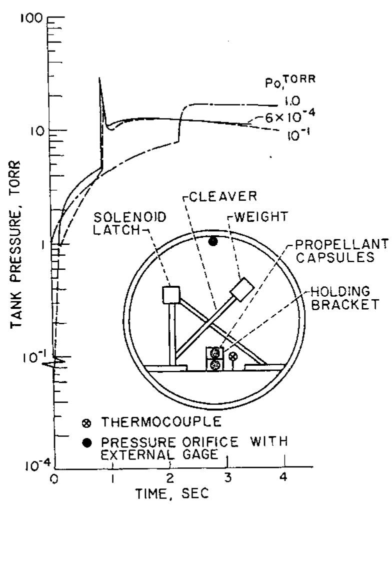

Fig. 2 Tank pressure rise with varying initial pressure; total propellant volume = 19.5 cm^3.

Conclusions

1) An explosive reaction occurred only when a sufficient quantity of propellant was used to produce a vaporized mixture pressure greater than 4 Torr.

2) For the decade of initial ambient pressure from 10^{-1} to 1 Torr, the reaction changed from an explosion to a slower reaction, as evidenced by a decrease in the magnitude of the explosion pressure and an increase in the reaction delay time.

3) N_2O_4 vaporized more quickly than N_2H_4, and the temperature decrease due to vaporization was sufficient to cause freezing of a portion of the N_2H_4.

A General Formula for Stiffness Matrices of Structural Elements

G. C. Best
Fort Worth, Texas

In this note a method is shown for developing stiffness matrices of elements composed of continuous elastic material. Following the general plan of Ref. 2, a stress assumption is made and loads are taken as the resultants of these stresses integrated over the sides. In matrix notation the stress assumption can be expressed as

$$\sigma = Uk \tag{1}$$

where $\sigma = \text{col}(\sigma_x,\sigma_y,\sigma_z, \tau_{xy},\tau_{yz},\tau_{zx})$ is the stress vector (assuming three dimensions), $k = \text{col}(k_1, k_1, \ldots k_r)$ with each k a constant, and U is a matrix whose elements are easily integrated functions of x,y,z, (e.g., $x^{v_1}y^{v_2}z^{v_3}$ with the v_i integers or zero) so that each stress is assumed approximated by a linear combination of elementary functions chosen to satisfy the differential equations of equilibrium and the equations of compatibility.

Integrating stresses over the surface of the element yields

$$p = Vk \tag{2}$$

giving a relation between the applied load vector p and the vector k. The elements of V are constants determined by the limits of integration.

Let m be the order of the stiffness matrix of the supported element. The number r of constants in the stress assumption is taken to be greater than m. For any given loading, the constants that are therefore in excess are so adjusted as to minimize the function

$$\overline{W} = \frac{1}{2} \oint_S \bar{\sigma}^T \bar{\sigma} dS \tag{3}$$

where $\bar{\sigma} = \text{col}(\sigma_n,\tau_{n1},\tau_{n2})$ and $\sigma_n,\tau_{n1},\tau_{n2}$ are the normal and shearing stresses on the surface of the element of surface area S. Let the matrix T transform from x,y,z coordinates to surface coordinates. Then

$$\bar{\sigma} = T\sigma \tag{4}$$

Inserting Eqs. (1) and (4) in (3) gives

$$\overline{W} = \frac{1}{2} k^T \left(\oint_S U^T T^T T U dS \right) k = \frac{1}{2} k^T B k \tag{5}$$

where $B = (b_{\alpha,\beta})$, and the parenthesized part in Eq. (5) is an $r \times r$ matrix that can be evaluated by numerical integration.

The minimization of (5) holding the loads constant is an isoperimetric problem in the calculus of variations.[3] Hence

Received May 20, 1963.

one writes as the function to be minimized, for a unit load on the ith coordinate,

$$\varphi = \frac{1}{2}\sum_{\alpha,\beta} b_{\alpha,\beta}k_\alpha k_\beta + \sum_{\alpha,\beta} \lambda_\alpha(V_{\alpha,\beta}k_\beta - \delta_\alpha{}^i) \quad (6)$$

where $\lambda\alpha$ are Lagrange multipliers and $\delta_\alpha{}^i$ is the Kroneker delta. Setting the partials with respect to the k_γ and the λ_γ to zero gives, on noting that B is symmetrical,

$$\frac{\partial\varphi}{\partial k_\gamma} = \sum_{\alpha=1}^{r} b_{\alpha,\gamma}k_\alpha + \sum_\alpha \lambda_\alpha V_{\alpha\gamma} = 0 \qquad \gamma = 1, 2, \ldots r \quad (7)$$

$$\frac{\partial\varphi}{\partial\lambda_\gamma} = \sum_\beta V_{\gamma\beta}k_\beta - \delta_\gamma{}^i = 0 \quad (8)$$

Returning to matrix notation and letting $\Gamma = \text{col}(\lambda_1,\lambda_2, \ldots\lambda_r)$, transforms Eqs. (7) and (8) into

$$Bk^{(i)} + V^T\Gamma^{(i)} = 0 \quad (9)$$

$$e_i = Vk^{(i)} \quad (10)$$

where e_i is a column vector with a one in the ith place and zeros elsewhere. The superscript i has been added to the k and Γ to indicate that here the load $p = e_i$. Assuming that B is nonsingular, one now premultiplies (9) by B^{-1} and transposes, obtaining

$$k^{(i)} = -B^{-1}V^T\Gamma^{(i)} \quad (11)$$

Substituting this into Eq. (10) and premultiplying the result by $(VB^{-1}V^T)^{-1}$ and substituting $\Gamma^{(i)}$ into (11) gives

$$k^{(i)} = B^{-1}V^T(VB^{-1}V^T)^{-1}e_i = Me_i \quad (12)$$

By Ref. 1 the flexibility matrix of the supported element is

$$F_{ij} = \int_V \sigma_{(i)}{}^T\epsilon_{(j)}dV \quad (13)$$

where $\sigma_{(i)}$ is the stress vector at a point in the element caused by a unit load at coordinate i, and $\epsilon_{(j)} = \text{col}(\epsilon_x{}^i,\epsilon_y{}^i,\epsilon_z{}^i,\gamma_{xy}{}^i, \gamma_{yz}{}^j,\gamma_{zx}{}^i)$ is the strain vector caused by unit load at j, the integration being taken over the volume V of the element. Expressing the customary relation between stress and strain in matrix notation as

$$\epsilon = N\sigma \quad (14)$$

and using Eqs. (1) and (12) converts Eq. (13) into

$$F_{ij} = e_i{}^TM^TGMe_j \quad \text{where} \quad G = \int_V U^TNUdV \quad (15)$$

This amounts to

$$F = M^TGM \quad (16)$$

By inversion of Eq. (16) one obtains the $m \times m$ stiffness matrix of the supported element:

$$\bar{S} = F^{-1} \quad (17)$$

In order to obtain the $n \times n$ stiffness matrix S of the unsupported element, the transformation matrix H is defined satisfying

$$\begin{pmatrix} p \\ p_F \end{pmatrix} = Hp \quad (18)$$

where p_F = support loads determined from equilibrium equations as linear combinations of the applied loads so that

$$S = H\bar{S}H^T \quad (19)$$

In order to show the nonsingularity of the matrices just inverted, Eq. (3) can be written as

$$\bar{W} = \frac{1}{2}\oint_S (\sigma_n{}^2 + \tau_{n1}{}^2 + \tau_{n2}{}^2)dS \quad (20)$$

which will be greater than zero unless $\sigma_n = \tau_{n1} = \tau_{n2} = 0$ everywhere, in which case $k = 0$. This amounts to saying that B is positive definite in Eq. (5) and hence nonsingular. Again, V in Eq. (2) should be of rank m, i.e., the loads should be independent, and therefore $V\ B^{-1}V^T$ is also of rank m and consequently nonsingular. For a unit load on the ith coordinate, the corresponding $k^{(i)}$ in Eq. (12) will not be zero, since M has rank m. The strain energy stored in the element is

$$\bar{U} = \frac{1}{2}\oint_V \epsilon_{(i)}{}^T\sigma_{(i)}dV = k^{(i)T}Gk^{(i)} \quad (21)$$

This can be zero only if the load is zero; hence $k = 0$. In other words G is positive definite and hence nonsingular.

References

[1] Argyris, J. H., "Energy theorems and structural analysis," Aircraft Eng., 43 (February 1955).

[2] Best, G., "A formula for certain types of stiffness matrices of structural elements," AIAA J. **1**, 212–213 (1963).

[3] Weinstock, R., *Calculus of Variations* (McGraw-Hill Book Co. Inc., New York, 1952), 1st ed., p. 48.

Support Interference Effects on the Supersonic Wake

BAIN DAYMAN JR.*

Jet Propulsion Laboratory, California Institute of Technology, Pasadena, Calif.

As it is generally recognized that the presence of a sting, no matter how feasibly small, is likely to affect base pressure and base heating, the use of side-mounted or wire-supported models is usually relied upon in order to obtain essentially disturbance-free measurements in the base region. During the development of the free-flight testing technique in the Jet Propulsion Laboratory continuous wind tunnels,[1] it was observed that the small diameter wires (used to support the models prior to their free-flight trajectories) usually had a significant effect upon the shape of the wake separation region. The purpose of this article is to demonstrate that the use of either side-mounts or wires to support a model in order to obtain interference-free base region measurements is not necessarily an adequate approach.

Concurrent with the acquisition of free-flight model-wake spark-chlieren pictures,[2] interference effect of small diameter-wire supports (0 to 3% of model diameter) upon the separation region shape was investigated for spheres and various cone models through the Mach number M range from M = 1.3 to M = 5 and for several cones at M = 9. The presence of a single traverse vertical wire support did alter noticeably the sphere separation region shape at $1.3 < M < 5$. Spark schlieren pictures at M = 3 in Fig. 1a indicate this typical interference effect. As the diameter of the vertical wire was increased from zero (free-flight) to 0.040 in., the position of the wake neck moved toward the sphere. Figure 1b is a graphical presentation of this wake interference phenomenon at several Reynolds numbers; the definition of the characteristic wake length, L, being shown in Fig. 1c. From these results it appears that any wire capable of supporting a sphere will alter the wake.

In Fig. 1a the schlieren pictures indicate that the flow field in the plane of the wire support has no obvious major dis-

Received May 14, 1963.

* Assistant Chief, Aerodynamic Facilities Section. Associate Fellow Member AIAA.